Semiclassical description of shell effects in finite fermion systems

Matthias Brack

Institute for Theoretical Physics, University of Regensburg,
D-93040 Regensburg, Germany

Abstract. Since its first appearance in 1971, Gutzwiller's trace formula has been extended to systems with continuous symmetries, in which not all periodic orbits are isolated. In order to avoid the divergences occurring in connection with symmetry breaking and orbit bifurcations (characteristic of systems with mixed classical dynamics), special uniform approximations have been developed. We first summarize some of the recent developments in this direction. Then we present applications of the extended trace formulae to describe prominent gross-shell effects of various finite fermion systems (atomic nuclei, metal clusters, and a mesoscopic device) in terms of the leading periodic orbits of their suitably modeled classical mean-field Hamiltonians.

1 Introduction

Although Gutzwiller investigated also integrable systems such as the Kepler problem in his series of papers [1] beginning in the late 1960s, the break through of his semiclassical theory came with the trace formula for isolated orbits, published in the last paper, whose 30th anniversary we are celebrating this year. This trace formula is most suited for chaotic systems in which all periodic orbits are unstable. It has, indeed, launched the success of the periodic orbit theory (POT) for the semiclassical description of chaotic systems [2,3,4,5]. Shortly after Gutzwiller, Balian and Bloch [6] published a trace formula for particles in two- and three-dimensional billiards with ideally reflecting walls, which may be integrable or non-integrable. The spherical cavity investigated by them found a beautiful physical realization in the 'supershell' structure of metal clusters [7] (see also [8]). Berry and Tabor first derived [9] a general trace formula for integrable systems starting from EBK quantization – a precursor of their approach may be found in [10] – and then showed [11] that it could also be derived from Gutzwiller's semiclassical Green function.

However, most physical systems are neither integrable nor chaotic, but have mixed classical dynamics. When a continuous (dynamical or spatial) symmetry is present, the periodic orbits appear in degenerate families and are no longer isolated. Starting in 1975, Strutinsky and collaborators [12] generalized Gutzwiller's approach to take into account such symmetries by performing some of the trace integrations exactly (instead of using the stationary-phase approximation). These authors also pioneered the idea of employing the

POT not for semiclassical quantization but for describing *gross-shell quantum effects* in mean-field systems in terms of their *shortest periodic orbits* [12,13]. For that purpose they derived trace formulae not only for the level density, but also for the energy shell-correction δE (i.e., the oscillating part of the total energy of an interacting system; see also [14] for details). A more general, and mathematically quite elegant, technique of deriving trace formulae for systems with continuous symmetries (including integrable systems) was developed in the early 1990s by Creagh and Littlejohn [15]. They transformed (part of) the trace integral in the phase-space representation to an analytical integration over the Haar measure of the symmetry group that characterizes the degenerate orbit families.

With this, trace formulae are available covering all situations from fully integrable to fully chaotic systems. The leading amplitudes in a trace formula (i.e., those with the lowest order in $\hbar$) come from the most degenerate orbit families [12,15]; less degenerate orbits contribute at higher orders in $\hbar$. This leads us to the next problem: when the variation of a continuous system parameter (energy, deformation, strength of an external field, etc.) causes the breaking or restoring of a symmetry, the leading-order amplitudes change discontinuously and diverge at the critical points. The same happens when periodic orbits undergo bifurcations, which is inevitable in a system with mixed dynamics. Both phenomena are closely related and, technically speaking, come from the break down of the stationary-phase approximation at the critical points. These divergences can be removed by going beyond the first-order saddle-point approximation [6], which results in local uniform approximations [16]. In order to recover the Gutzwiller amplitudes far from the critical points, global uniform approximations must be developed.

In this paper we first review briefly some uniform approximations, without discussing any technical details, and present two recent examples (Sect. 2). We then give in Sect. 3 a personal account of some applications of the POT to the semiclassical description of gross-shell effects in various finite fermion systems (nuclei, metal clusters, and a mesoscopic device) in terms of the leading periodic orbits of their modeled mean-field Hamiltonians.

2 Uniform approximations for symmetry breaking and bifurcations

Uniform approximations can most elegantly be derived using normal forms of the action integral in the exponent of the semiclassical Green function in the phase-space representation [16]. Tomsovic *et al.* [17] derived a general trace formula for the generic breaking of periodic orbit families in two-dimensional systems with U(1) symmetry into isolated pairs of stable and unstable orbits. Starting from the Berry-Tabor trace formula [9] in the integrable limit, they generalized the local uniform approximation of Ozorio de Almeida and Hannay [16] by means of a non-linear coordinate transformation, expanding the

Jacobian of this transformation and the Van Vleck determinant consistently with the expansion of the action integral in the semiclassical Green function, and matching the asymptotic Gutzwiller amplitudes and actions of the isolated orbits away from the integrable limit. No generally valid trace formula for the breaking of higher symmetries have been found so far.

Special uniform approximations for the breaking of SU(2) symmetry in two-dimensional systems and SO(3) symmetry in a three-dimensional system with axial symmetry have been derived by Brack *et al.* [18]. In Fig. 1 we show their result for the coarse-grained level density of the well-known Hénon-Heiles potential [19] which has become a paradigm for a system with mixed dynamics reaching from near-integrable motion at low energy up to nearly chaotic motion at the scaled critical energy (normalized to $e = 1$) at which the particle can escape over a saddle. An excellent agreement between quantum mechanics and semiclassics is reached up to about 75% of the critical energy. At low energies, one reaches the SU(2) symmetry of the two-dimensional isotropic harmonic oscillator with its regular shell structure (frequency ω) and an amplitude linear in the energy (see [14]). In the region $0.3 < e < 0.75$, the original Gutzwiller trace formula for isolated orbits applies [20], and the uniform approximation is seen here to interpolate smoothly down to the integrable limit at $e = 0$. The break down at $e > 0.75$ is mainly due to bifur-

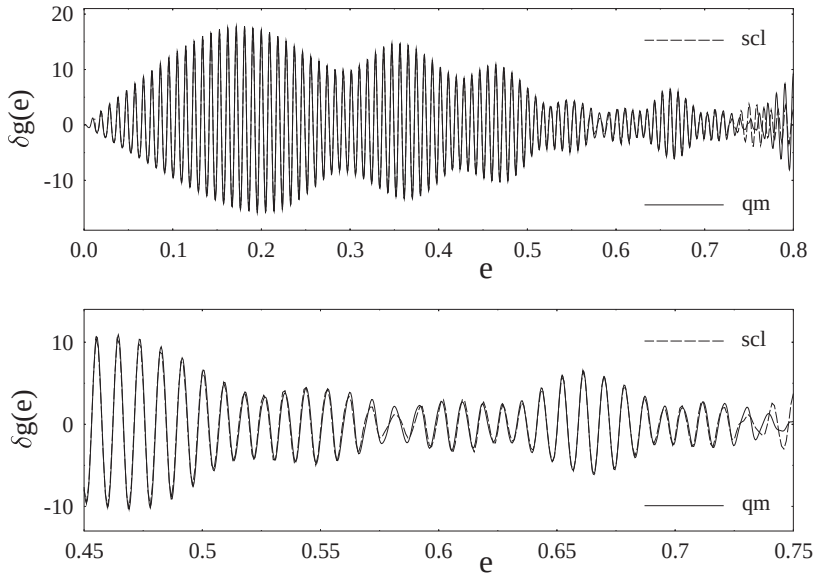

Fig. 1. Level density of the Hénon-Heiles potential, Gaussian convoluted over an energy interval $\gamma = 0.25\,\hbar\omega$. *Solid line:* quantum result. *Dashed line:* semiclassical result in the uniform approximation of [18]; only the three shortest primitive orbits and their second repetitions are included.

cations. The straight-line orbit approaching the saddle undergoes an infinite cascade of isochronous bifurcations which coalesce at the critical energy $e = 1$ and pose a series problem to their semiclassical treatment. (See also [21], where the self-similarity and Feigenbaum type scaling properties of the bifurcated orbits are discussed analytically.)

The most systematic development of uniform trace formulae for all generic types of bifurcations has been undertaken by Sieber and Schomerus [22], who also used local normal forms and extended them in order to smoothly join the asymptotic Gutzwiller amplitudes of the isolated orbits as sketched above. Hereby also the analytical continuations of periodic orbits into the complex phase space (so-called 'ghost orbits' [23]) contribute in the neighborhood of the bifurcations. Interferences of close-lying bifurcations (of codimension two) [24] and bifurcations of ghost orbits [25] have also been successfully treated with the same technique.

In [26], an analytical trace formula has been derived for the two-dimensional ellipse billiard. Although this is an integrable system, it exhibits all the complications of mixed systems, including symmetry breaking and bifurcations. Figure 2 shows in a contour plot (a) its coarse-grained oscillating level density $\delta g(E)$ versus wave number k and axis ratio η. Next to it (b) we see the lines of constant actions of the shortest periodic orbits illustrated on the right-hand side. The standard uniform approximations were not used in [26];

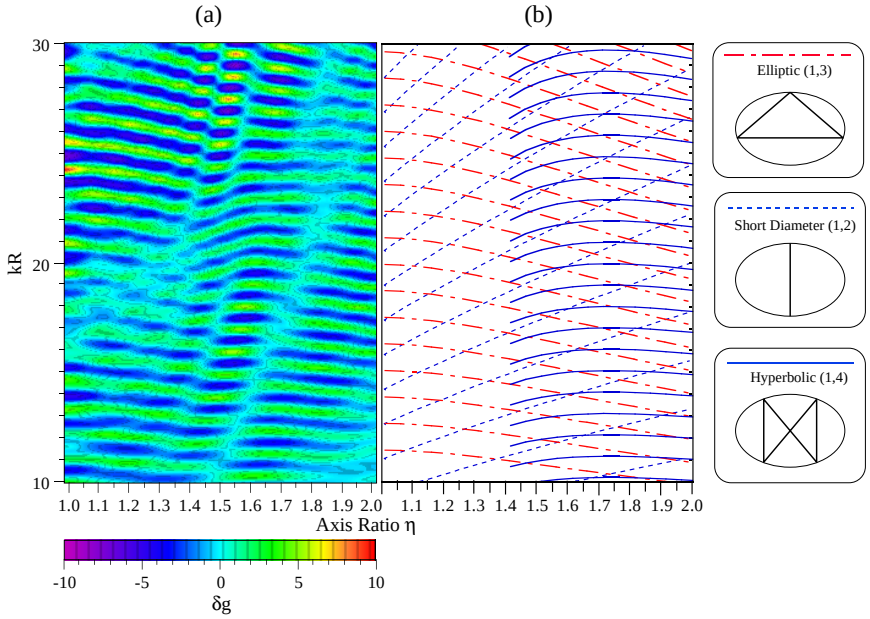

Fig. 2. Contour plot of level density in the ellipse billiard (a) and loci of constant actions (b) of its leading periodic orbits. (See text and [26] for details.)

the divergences in the spherical limit and at the bifurcations of the short diameter orbit (i.e., of its repetitions) could be removed by limiting the lowest-order saddle-point integration to the finite limits imposed by the classically allowed region. Note that the shell structure seen on the left of Fig. 2 in some regions of the (k, η) plane is clearly affected by the onset of the new hyperbolic 'bow-tie' orbit familiy born in a bifurcation at $\eta = \sqrt{2}$. An extension of this study to the three-dimensional spheroidal cavity is in progress [27].

A simple, but efficient way to avoid the difficulties connected with symmetry breaking and bifurcations, at least in some situations, is to use a perturbative trace formula developed by Creagh [28]. In this approach which, of course, can only be used for sufficiently small deviations from an integrable limit, the effect of a non-integrable perturbation is only taken into account in the actions of the periodic orbits; the stability amplitudes and Maslov indices of the integrable system are kept unchanged. (A similar approach was used also in [29].) This results in the modification of the integrable-limit trace formula merely by a modulation factor which contains the average of the lowest non-vanishing perturbation of the action over each unperturbed orbit family, and which often can be calculated analytically [28,30,31]. An application of the perturbative trace formula is given in Sect. 3.1 below.

3 Applications to shell structure in finite fermion systems

3.1 Ground-state deformations of nuclei and metal clusters

An early application of the POT to explain the systematics of ground-state deformations of atomic nuclei was given by Strutinsky *et al.* [13]. In contour plots of the quantum-mechanically calculated energy shell-correction δE versus nucleon numbers N and deformation parameter η, the correct slopes of the minimum valleys are reproduced by the systematics predicted from the leading periodic orbits of a spheroidal cavity. A more complete study in the same model was given later by Frisk [32], and a detailed Fourier analysis of its quantum spectrum was performed by Arita *et al.* [33], who also discussed the role of orbit bifurcations (without, however, developing the appropriate trace formulae). All these authors have neglected the spin-orbit interaction; although it is known to modify the shell structure in nuclei (cf. Fig. 4), its effect could be simulated by a simple renormalization of the Fermi energy (see also Sect. 3.2 below).

Luckily, the ground-state deformations of not too light nuclei and metal clusters are sufficiently small so that the perturbative trace formula of Creagh [28] may be applied successfully. In Fig. 3 we show a recent comparison of the lowest multipole deformations of sodium clusters, calculated [34] both quantum-mechanically and semiclassically with the perturbative trace formula using the modulation factors derived in [30]. The total energy of each cluster with fixed particle number N was minimized with repect to all three

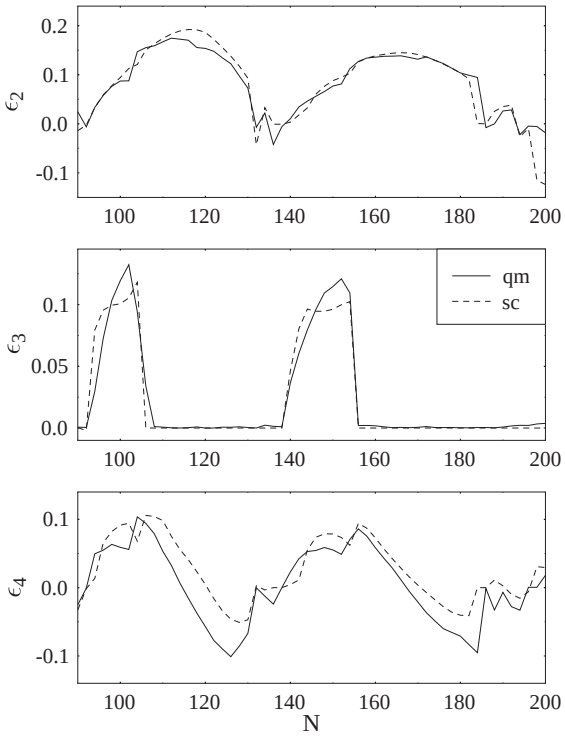

Fig. 3. Ground-state quadrupole (ϵ_2), octopole (ϵ_3), and hexadecapole (ϵ_4) deformations of sodium clusters versus number N of valence electrons, using axially deformed cavities as their mean potential. *Solid lines:* quantum results. *Dashed lines:* semiclassical results using the perturbative trace formula [28,30]. (From [34].)

deformation parameters. Their equilibrium values obtained in the two ways are seen to agree almost quantitatively, which demonstrates the usefulness of the perturbative semiclassical approach. Note that the spin-orbit interaction plays a negligible role in sodium clusters [8].

As a first step towards the inclusion of the spin-orbit interaction in the semiclassical trace formula for nuclei, we show in Fig. 4 the level density obtained recently [35] for a three-dimensional deformed harmonic oscillator which is a realistic model for light nuclei. Hereby the approach of Littlejohn and Flynn [36] was employed in the same heuristic way as in [37]. Instead of giving more details of this approach, we refer to a more rigorous semiclassical theory including spin degrees of freedom [38]. We see in Fig. 4 that the spin-orbit interaction does drastically change the gross-shell structure, and that it can be described semiclassically, indeed. In the present example the still unsolved mode-conversion problem (occurring along manifolds in phase space where the spin-orbit interaction locally is zero) did not arise. Some steps towards its solution in a two-dimensional system are in progress [39].

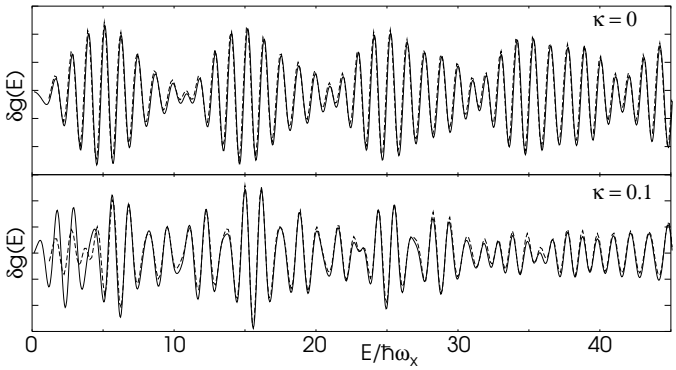

Fig. 4. Coarse-grained level density of a three-dimensional harmonic oscillator with frequencies $\omega_x = 1$, $\omega_y = 1.12128$, $\omega_z = 1.25727$ (Gaussian averaging range $\gamma = 0.2\,\hbar\omega_x$), both without (top) and including a spin-orbit interaction (bottom). *Solid lines:* quantum-mechanical, *dotted lines:* semiclassical results (see [35] for details).

3.2 Mass asymmetry in nuclear fission

Another example for the contribution of periodic orbits to a prominent quantum shell effect in a complex interacting fermion system is the asymmetry in the fission of heavy nuclei, which results in an asymmetric distribution of the fission fragments. This asymmetry, which sets in already during the passage over the saddle in the deformation energy space, has long been taken as a prime example of a quantum phenomenon that could not be explained classically, e.g., in terms of the liquid-drop model. (For a detailed presentation of the role of shell effects in nuclear fission see, e.g., the review [40].) The POT, however, allows to understand this effect semiclassically, using only very few periodic orbits [41,42]. Figure 5 shows a pespective view of the deformation energy of a typical heavy nucleus, plotted versus elongation parameter c and asymmetry parameter α. It was calculated in [41] using the trace formula for

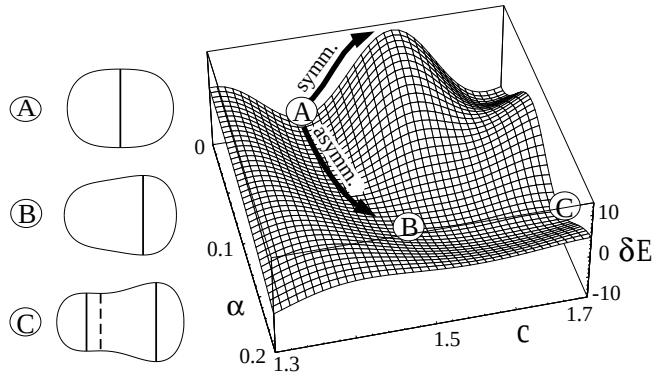

Fig. 5. Fission barrier of a heavy nucleus. (From [41]; see text for details.)

the shell-correction energy δE of particles in an axially deformed cavity with the shapes defined in [40]. A coarse-graining simulating the pairing interaction was used. The lowest adiabatic path to fission, determined by the stationarity of the actions of the leading orbits (cf. [13]), leads from the isomer minimum (point A) over a saddle with asymmetric shapes ($\alpha > 0$, points B and C). Imposing symmetry ($\alpha = 0$) would lead over a barrier at appreciably higher energy. This is exactly the topology of the fission barrier obtained in the old quantum-mechanical calculations with realistic nuclear shell-model potentials [40]. Only few periodic orbits need to be included to obtain the semiclassical result. They lie in planes perpendicular to the symmetry (z) axis, as illustrated to the left of Fig. 5 by the perpendicular lines (solid for stable and dashed for unstable orbits) drawn into the shapes corresponding to the three points in deformation space. These orbits are just the polygons inscribed into the circular cross sections of the cavity with those planes; their stability amplitudes were given by Balian and Bloch [6]. A uniform approximation was used in [41] to handle the bifurcation happening when the cavity starts to neck in and the plane containing the shortest orbits splits into three planes (existing, e.g., at point C). As shown in [42], only primitive orbits with up to ~ 5 reflections were needed in each plane to obtain a converged result; the two shortest orbits (diameter and triangle) were, in fact, sufficient to obtain the correct topology of the asymmetric fission barrier. As in [13,32], the spin-orbit interaction was neglected; instead, the Fermi energy was adjusted such that the isomer minimum appeared at the correct deformation.

It is interesting to notice that the classical motion in the cavities with shapes occurring around the fission barrier is quite chaotic, as discussed in more detail in [43]. In Fig. 6 we show a Poincaré surface of section, taken at the asymmetric saddle (near point B) for a number of trajectories starting from random initial conditions with angular momentum $L_z = 0$. It reveals us

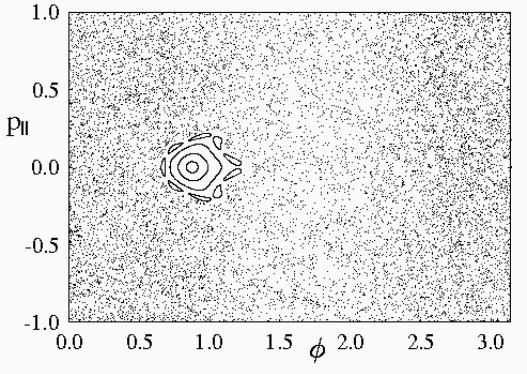

Fig. 6. Poincaré surface of section of classical trajectories with $L_z = 0$ at deformation of asymmetric saddle (B). At each mapping (reflection off the boundary), ϕ is the polar angle and $p_{||}$ the momentum component parallel to the tangent plane.

that this part of the phase space is, indeed, more than 95% chaotic. Only a small regular island surrounds the fixed point corresponding to the diameter orbit. It is this small regular island, embedded in a chaotic phase space, that hosts the periodic orbit which is chief responsible for the shell effect driving the nucleus to asymmetric shapes. In the microscopic description, the quantum-mechanical states responsible for this shell effect are a few 'diabatic' states whose eigenenergies depend strongly on the asymmetry parameter, causing the energy gain in going from the symmetric to the asymmetric saddle, whereas most other states are insensitive to it (cf. [44]). The diabatic quantum states in the present cavity model were shown in [43] to have their probability maxima exactly in the planes containing the shortest periodic orbits. Furthermore, an approximate EBK quantization of the classical motion near those planes reproduces the eigenergies of the diabatic quantum states almost quantitatively [43], thus establishing a nice quantum-to-classical correspondence in a highly nonlinear complex system.

3.3 Mesoscopic systems

We finally turn to a mesoscopic arrangement in which a two-dimensional electron gas is confined laterally to a channel of width $\sim 1.0\,\mu$m. Two antidots represent obstacles to the electric current through the channel; the effective radius of these antidots can be regulated by an applied gate voltage V_g. Figure 7 shows an SEM photograph of the experimental gate structure [45]. The longitudinal conductance G_{xx} along the channel was measured for various strengths of a perpendicular magnetic field B and various gate voltages V_g [45,46]. A commensurability minimum in the average conductance was observed near those values of B for which a cyclotron orbit fits around the antidots. Small observed oscillations around the average part of G_{xx} could be interpreted semiclassically [47,48] by the interferences of the leading periodic orbits (a few of which are shown in Fig. 7 by solid and dashed white lines). In Fig. 8 we compare the experimental oscillations δG_{xx} with the result of the calculation [48] in which the semiclassical Kubo formula [49] was used.

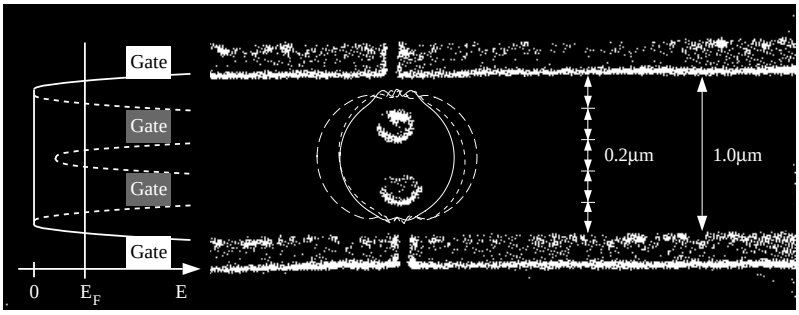

Fig. 7. Mesoscopic channel with two antidots (from [47]). *Left:* sketch of the model potential confining the electrons, and position of the Fermi energy E_F.

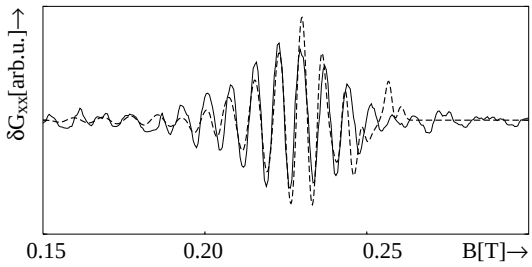

Fig. 8. Comparison of experimental conductance oscillations (solid line) and semiclassical result (dashed line) with optimized parameters of the model potential [48].

An interesting phenomenon is observed when varying both the magnetic field B and the gate voltage V_g and plotting the loci of the oscillation maxima in δG_{xx}. These arrange themselves, as seen in Fig. 9 (a), along smooth lines whose slopes are well understood in terms of the B and V_g dependence of the actions of the leading periodic orbits. However, some characteristic dislocations occur at apparently random places in the (B, V_g) plane, as emphasized by the boxes. In the semiclassical analysis, they originate from successive bifurcations of periodic orbits: the different orbit generations lead to different slopes in Fig. 9 (b), and these do not match near the loci in the (B, V_g) plane (shown for some leading orbits by gray-shaded thick lines) along which the bifurcations occur. Although the theory does not fit the experiment globally

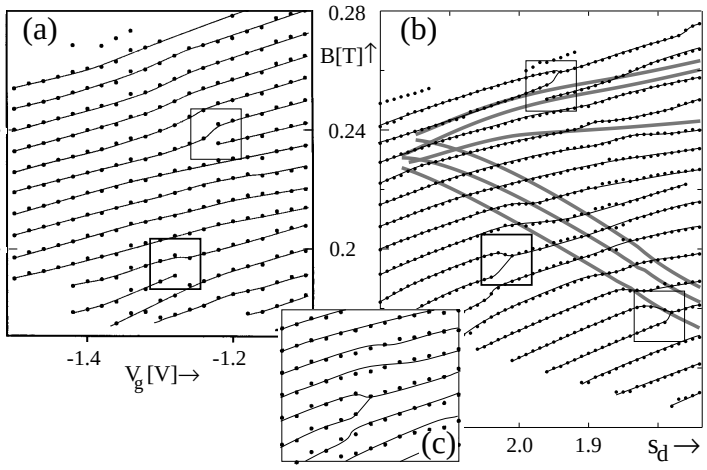

Fig. 9. Maximum positions of δG_{xx} versus B (vertical axes) and V_g (horizontal axes). (a) Experimental values [46]. (b) Semiclassical results [47]; s_d is the antidot radius regulated by V_g (approximately one has $s_d \propto V_g$); the gray-shaded lines correspond to the loci of bifurcations of some leading orbit families. (c) Behaviour near a dislocation (dots: experiment; lines: semiclassical results). (From [47].)

(at least 10 different orbit families contribute), the local agreement near the dislocations is excellent; see the box in Fig. 9 (c). A quantum-mechanical calculation [46] qualitatively reproduced the dislocations, too. But the physical understanding of their origin required the semiclassical analysis in terms of periodic orbits. As we see, even the orbit bifurcations have experimentally observable consequences!

I am grateful to all my students and collaborators whose work has been presented here, and to the Deutsche Forschungsgemeinschaft for partial financial support.

References

1. M. C. Gutzwiller, J. Math. Phys. **12**, 343 (1971); and earlier references quoted therein
2. M. C. Gutzwiller: *Chaos in classical and quantum mechanics* (Springer, New York, 1990)
3. *Chaos Focus Issue on Periodic Orbit Theory*, Chaos, Vol. 2, No. 1 (1992)
4. *Quantum Chaos Y2K*, Proceedings of Nobel Symposium 116, K.-F. Berggren and S. Åberg (Eds.), Physica Scripta Vol. **T90** (2001)
5. see also most other contributions to this symposium
6. R. Balian, and C. Bloch, Ann. Phys. (N. Y.) **69**, 76 (1972)
7. H. Nishioka, K. Hansen, and B. R. Mottelson, Phys. Rev. B **42**, 9377 (1990) J. Pedersen, S. Bjørnholm, J. Borggreen, K. Hansen, T. P. Martin, and H. D. Rasmussen, Nature **353**, 733 (1991)
8. M. Brack, Rev. Mod. Phys. **65**, 677 (1993)
9. M. V. Berry and M. Tabor, Proc. R. Soc. Lond. A **349**, 101 (1976)
10. E. N. Bogachek and G. A. Gogadze, Sov. Phys. JETP **36**, 973 (1973)
11. M. V. Berry and M. Tabor, Proc. R. Soc. Lond. A **356**, 375 (1977)
12. V. M. Strutinsky, Nukleonika (Poland) **20**, 679 (1975) V. M. Strutinsky and A. G. Magner, Sov. J. Part. Nucl. **7**, 138 (1976)
13. V. M. Strutinsky, A. G. Magner, S. R. Ofengenden, and T. Døssing, Z. Phys. A **283**, 269 (1977)
14. M. Brack and R. K. Bhaduri: *Semiclassical Physics*, Frontiers in Physics Vol. 96 (Addison-Wesley, Reading, USA, 1997)
15. S. C. Creagh and R. G. Littlejohn, Phys. Rev. A **44**, 836 (1991) S. C. Creagh and R. G. Littlejohn, J. Phys. A **25**, 1643 (1992)
16. A. M. Ozorio de Almeida and J. H. Hannay, J. Phys. A **20**, 5873 (1987) see also A. M. Ozorio de Almeida: *Hamiltonian Systems: Chaos and Quantization* (Cambridge University Press, Cambridge, 1988)
17. S. Tomsovic, M. Grinberg, and D. Ullmo, Phys. Rev. Lett. **75**, 4346 (1995) D. Ullmo, M. Grinberg, and S. Tomsovic, Phys. Rev. E **54**, 135 (1996)
18. M. Brack, P. Meier, and K. Tanaka, J. Phys. A **32**, 331 (1999)
19. M. Hénon and C. Heiles, Astr. J. **69**, 73 (1964)
20. M. Brack, R. K. Bhaduri, J. Law, M. V. N. Murthy, and Ch. Maier, Chaos **5**, 317 (1995); Erratum: Chaos **5**, 707 (1995)

21. M. Brack, in: *Festschrift in honor of the 75th birthday of Martin Gutzwiller*, A. Inomata *et al.* (Eds.), Foundations of Physics **31**, 209 (2001); LANL preprint nlin.CD/0006034
22. M. Sieber, J. Phys. **A 29**, 4715 (1996)
    H. Schomerus and M. Sieber, J. Phys. A **30**, 4537 (1997)
    M. Sieber, J. Phys. A **30**, 4563 (1997)
    M. Sieber and H. Schomerus, J. Phys. A **31**, 165 (1998)
23. M. Kuś, F. Haake, and D. Delande, Phys. Rev. Lett. **71**, 2167 (1993)
24. H. Schomerus, Europhys. Lett. **38**, 423 (1997); J. Phys. A **31**, 4167 (1998)
    J. Main and G. Wunner, Phys. Rev. A **55**, 1753 (1997)
    J. Main and G. Wunner, Phys. Rev. E **57**, 7325 (1998)
25. T. Bartsch, J. Main, and G. Wunner, Ann. Phys. (N.Y.) **277**, 19 (1999)
26. A. Magner, S. N. Fedotkin, K. Arita, T. Misu, K. Matsuyanagi, T. Schachner, and M. Brack, Prog. Theor. Phys. (Japan) **102**, 551 (1999)
27. A. G. Magner, S. N. Fedotkin, K. Arita, K. Matsuyanagi, and M. Brack, Phys. Rev. A (2001), in press; LANL preprint nlin.SI/0101035
    A. G. Magner *et al.*, to be published
28. S. C. Creagh, Ann. Phys. (N. Y.) **248**, 60 (1996)
29. D. Ullmo, K. Richter, and R. A. Jalabert, Phys. Rev. Lett. **74**, 383 (1995)
    K. Richter, D. Ullmo, and R. A. Jalabert, Phys. Rep. **276**, 1 (1996)
30. P. Meier, M. Brack, and S. C. Creagh, Z. Phys. D **41**, 281 (1997)
31. M. Brack, S. C. Creagh, and J. Law, Phys. Rev. A **57**, 788 (1998)
32. H. Frisk, Nucl. Phys. A **511**, 309 (1990)
33. K. Arita, A. Sugita, and K. Matsuyanagi, Prog. Theor. Phys. **100**, 1223 (1998)
34. V. V. Pashkevich, P. Meier, M. Brack, and A. V. Unzhakova, Regensburg preprint TPR-00-24 (2000)
35. M. Brack and Ch. Amann, in: *International Workshop on Fission Dynamics of Atomic Clusters and Nuclei*, D. Brink *et al.* (Eds.) (World Scientific Publishing, Singapore, 2001), in press; LANL preprint nucl-th/0010047
36. G. Littlejohn and W. G. Flynn, Phys. Rev. A **44**, 5239 (1991)
37. H. Frisk and T. Guhr, Ann. Phys. (N. Y.) **221**, 229 (1993)
38. J. Bolte and S. Keppeler, Ann. Phys. (N. Y.) **274**, 125 (1999)
    see also J. Bolte, Adv. Solid State Phys. (this volume)
39. M. Pletyukhov, M. Mehta, and Ch. Amann, to be published
40. M. Brack, J. Damgård, A. S. Jensen, H. C. Pauli, V. M. Strutinsky, and C. Y. Wong, Rev. Mod. Phys. **44**, 320 (1972)
41. M. Brack, S. M. Reimann, and M. Sieber, Phys. Rev. Lett. **79**, 1817 (1997)
42. M. Brack, P. Meier, S. M. Reimann, and M. Sieber, in: *Similarities and differences between atomic nuclei and clusters*, Y. Abe *et al.* (Eds.) (American Institute of Physics, 1998) p. 17
43. M. Brack, M. Sieber, and S. M. Reimann, in [4], p. 146
44. C. Gustafsson, P. Möller, and S. G. Nilsson, Phys. Lett. **34 B**, 349 (1971)
45. C. Gould *et al.*, Phys. Rev. B **51**, 11213 (1995)
46. G. Kirczenov *et al.*, Phys. Rev. B **56**, 7503 (1997)
47. J. Blaschke and M. Brack, Europhys. Lett. **50**, 294 (2000)
48. J. Blaschke, Ph. D. Thesis, Regensburg University, 1999
    available at ⟨http://www.joachim-blaschke.de⟩
49. K. Richter, Europhys. Lett. **29**, 7 (1995)
    G. Hackenbroich and F. von Oppen, Europhys. Lett. **29**, 151 (1995)